# Composites Made From a Soybean Oil Biopolyurethane and Cellulose Nanocrystals

AQ6 Veronica L. Mucci,[1] Aiga Ivdre,[2] Juan M. Buffa,[1] Ugis Cabulis,[2] Pablo M. Stefani,[1] Mirta I. Aranguren[1]

*[1] Instituto de Investigación en Ciencia y Tecnología de Materiales (INTEMA), UNMDP, CONICET, Facultad de* AQ1 *Ingeniería, Av. Juan B Justo 4302, Mar del Plata 7600, Argentina*

*[2] Polymer Laboratory, Latvian State Institute of Wood Chemistry, 27Dzerbenes, Riga LV-1006, Latvia*

**Cellulose nanocrystals (CNC) obtained by acidic hydrolysis from microcrystalline cellulose were dispersed in a biopolyurethane matrix to prepare composite films. The polyurethane was prepared from a hydroxylated soybean oil (SO-OH) and a polymeric diphenyldiisocyanate (pMDI), using a tertiary amine as the catalyst. The composite films contained different concentrations of nanocelullose, without any macroscopic aggregates in all cases. Thermal, tensile and dynamic mechanical properties of the films were determined for all the samples. In particular, it was observed that the glass transition temperature of the nanocomposites slightly increased with the concentration of the cellulose nanocrystals. The nanocomposite with 1 wt% of nanocellulose showed the highest tensile strength of the series.** POLYM. ENG. SCI., 00:000–000, 2017. © 2017 Society of Plastics Engineers

## INTRODUCTION

There is an increasing interest in the preparation of polymers from renewable resources, i.e. bio-based polymers derived from living organism like plants, trees and algae, due to the declining of non-renewable feedstock. The use of renewable resources in the formulation of materials has attracted great attention in both industrial and academic fields because of environmental reasons besides sustainability [1–3]. Bio-based polymers have also numerous benefits such as their abundant availability, low price and their environmentally benign nature. Two major renewable resources available in large volumes are cellulose and vegetable oils. The use of cellulose in polymeric coatings is not very common, while vegetable oils are used mostly to prepare polymeric binders for coating formulations, resin applications and flooring materials. Fats and oils of animal and vegetable origins have a long history of being one of the most important renewable raw materials used in the industrial synthesis of fine chemicals. In particular, vegetable oils can be converted into derivatives and polymer precursors, for instance, alkyd resins and alkyd based-polyols [4].

Bio-based polyols are increasingly used in the formulation of polyurethanes (PUs). This family of polymers has become one of the most widely used plastics for various applications such as thermal insulation, construction, automotive parts and seating materials, in forms of rigid, semirigid, and flexible foams as well as elastomers. Polyols that are reacted with different diisocyanates to obtain PUs, are derived mostly from petrochemical products but can be replaced by renewable materials. Therefore, polyurethanes have been synthesized from bio-polyols derived from vegetable oils obtained from various plant seeds such as castor bean [5–7], cotton, rapeseed [8–11], jatropha, palm [12, 13], soybean [14, 15], and sunflower [11, 16].

In addition, different natural fillers have been used to improve the characteristics of rigid PUs, to reduce production costs and to increase the concentration of components from renewable resources in the final products [17]. In particular, different types of cellulose have been combined with PUs to prepare materials fitted for a large variety of applications [18–20]. Cellulose is a high molecular weight carbohydrate obtained mainly from plants, but also from some bacteria strains [21]. It constitutes the most abundant renewable polymer available in nature. Most of the studies found in the literature about biocomposites that incorporate cellulose report that it increases the rigidity, but usually embrittles the polymer [22]. Through different processes, cellulose can be separated into nanoscale entities [23–25]. The most usual process for the isolation of cellulose nanocrystals (CNC) from cellulose fibers consists on acid hydrolysis. This treatment followed by further washing of the fibers yields defect-free, rod-like crystalline particles usually called nanowhiskers or nanocrystals [23] that are being regarded as the next generation renewable reinforcement for the production of high performance biocomposites. CNCs have been the subject of a wide array of research efforts to introduce them as reinforcing agents in nanocomposites due to their low cost, availability, renewability, lightweight, nanoscale dimension, and unique morphology [1, 19, 26, 27].

The present work describes a method for obtaining nanocomposites prepared from a polyurethane based on a hydroxylated soybean oil with different concentrations of well dispersed CNCs. The physical, mechanical, and thermal properties of these nanocomposite films were investigated and the effect of the cellulose addition was analyzed.

## EXPERIMENTAL

### *Materials*

The synthesis of the biopolyurethane was based on the reaction of 4,4′-diphenylmethane diisocyanate prepolymer, pMDI (Rubinate 5005, Huntsman Polyurethanes, USA) with an equivalent weight of 131 g/eq and a hydroxylated soybean oil as the polyol component, Agrol 3.6 from Biobased Technologies, USA, with an OH value = 120.8 mg KOH/g (measured according to DIN 53240 norm). The reaction was catalyzed by dibutyltindilaurate (DBTDL) (Alkanos S.A. Co.). The CNC were prepared from the acid hydrolysis of a commercial

*Correspondence to:* V.L. Mucci; e-mail: vmucci@fi.mdp.edu.ar and M.I. Aranguren; e-mail: marangur@fi.mdp.edu.ar

Contract grant sponsor: BIOPURFIL Project; contract grant number: PIRSES-GA-2012-318996 by the EC through the FP7; contract grant sponsor: National Research Council of Republic Argentina (CONICET); contract grant number: PIP 0866; contract grant sponsor: Science and Technology National Promotion Agency (ANPCyT); contract grant number: PICT140732; contract grant sponsor: National University of Mar del Plata (UNMdP); contract grant number: 15/G430-ING436/15.

DOI 10.1002/pen.24539

Published online in Wiley Online Library (wileyonlinelibrary.com).

© 2017 Society of Plastics Engineers

microcrystalline cellulose from Sigma Aldrich (USA). Sulfuric acid and acetone (from Cicarelli, Argentina) were other reagents used in the preparation of the materials.

*Synthesis and Characterization of CNC*

To obtain the CNC, the acid hydrolysis of microcrystalline cellulose was carried out by mixing 15 g of microcrystalline cellulose and 52.5 g of distilled water in a flask under mechanical agitation. Then, 97.5 g of sulfuric acid (98 wt%) were added dropwise while the temperature of the mixture was maintained at 30°C; reaching a final acid concentration in the aqueous suspension of 64 wt%. After adding all the acid, the solution was heated to 44°C and the hydrolysis continued for 2 h more, under continuous stirring. Then, the solution was cooled down in refrigerator for 24 h. The resulting solution had a pH of 1 to 2, and was dialyzed against distilled water to remove any free acid molecules from the dispersion. A Spectra/Por molecular porous membrane with molecular weight cut-off range of 12,000 to 14,000 Da was used for the dialysis, which was continued until the pH reached a constant value of ~6. Finally, the solution was filtered to remove any remaining large aggregate.

The concentration of CNC in the suspension was determined by taking an aliquote and weighing the solids after drying. The average size of the particles was determined by dynamic light scattering (DLS) using an equipment Malvern Zetasizer Nano S-90 with a laser of 632 nm (Malvern Instruments Co. Ltd., Worcestershire, UK), at 25°C on highly diluted suspensions, prepared with deionized water. The refraction index of the disperse phase and the continuous phase were 1.00 and 1.33 respectively.

*Preparation of Nanocomposites*

To prepare the nanocomposites, a solvent exchange of the CNC suspension was performed. Thus, the aqueous suspension of CNC was centrifuged four times using a cycle of 30 min at 12,000 rpm. The supernatant obtained at the end of each cycle was removed and replaced with acetone. Once the solvent exchange was completed, the CNCs dispersed in acetone were mixed with the well dried biopolyol. To disperse the CNCs into the polyol and obtain a homogenous distribution of the crystals, a dispersing instrument IKA T 18 Basic Ultra-Turrax was used Acetone was then evaporated, initially for two days at room temperature, and afterwards by keeping the mixture in a vacuum oven for two more days at 40°C.

The nanocomposite samples were prepared by mixing the dispersion of the biopolyol and CNC with DBTDL (0.1 wt%) and pMDI at NCO/OH molar ratio of 1.2. The mixture was poured in a preheated mold (at 80°C), which was then closed and placed in a press at 0.5 MPa and 80°C for 2 h. After removal from the press, the mould was put in an oven at 80°C for 16 h. Finally, the samples (thickness 2.0± 0.2 mm) were conditioned at room temperature for a 24 h before cutting specimens for the different tests. Nanocomposites were prepared with CNC concentrations of 0, 0.5, 1.0, and 2.0 wt% with respect to the total weight of the sample.

*Characterization of Nanocomposites*

The samples were observed under cross polarized light to assess the overall distribution of the CNC by the birefringence of the sample.

Color parameters and opacity were determined using a Lovi Bond Colorimeter RT500 (Amesbury, United Kingdom) with an 8 mm diameter measuring area. The opacity is given as the percentage of light that does not pass through a material. Thus, the higher the opacity, the lower the amount of light that can pass through the material and the lower its transparency [28]. Film specimens were measured against the surface of a standard white plate, and the CIELAB color space was used to obtain the color coordinates. Lightness ($L^*$), redness ($a^*$), or greenness ($-a^*$), and yellowness ($b^*$) or blueness ($-b^*$) were determined. Whiteness index (WI) was calculated as given by Eq. *1* [29].Results were expressed as the average of three samples.

$$WI = 100 - \sqrt{(100 - L^*)^2 + a^{*2} + b^{*2}} \quad (1)$$

The images of the fracture surface of the composites (fracture performed under cryogenic conditions) were obtained with a JEOL scanning electron microscope, Model JSM-6460LV (Tokyo, Japan), with a secondary electron detector. An acceleration voltage of 15 kV, and different magnifications were used.

Attenuated total reflectance-Fourier transformed infrared (ATR-FTIR) spectra were obtained using a Thermo Scientific Nicolet 6700 spectrometer (Wisconsin, USA). The signal was recorded between 400 and 4,000 $cm^{-1}$ using an attenuated total reflectance accessory (ATR) with a diamond ATR crystal. A total of 32 scans were averaged at 8 $cm^{-1}$ resolution for each spectrum.

X-ray diffraction measurements were performed at a scanning speed of 0.016°$s^{-1}$ using a X PANalytical X′ Pert PRO X-ray diffractometer with Cu (Kα) radiation, covering a diffraction angle from 2° to 60°. The crystallinity of the samples was calculated as the ratio of crystalline to total areas.

Thermogravimetric analysis (TGA) measurements were carried out in a Shimadzu TGA-50 (Japan). The samples (5–7 mg) were heated from 25°C to 500°C at a heating rate of 10°C $min^{-1}$ under nitrogen and air atmospheres (20 mL $min^{-1}$) [30].

Dynamic mechanical analysis was performed in torsion mode using an Anton Paar Physica MCR 301 rheometer. A fixed frequency of 1 Hz and oscillation amplitude of 0.1% were used. Test specimens were rectangular cross-section bars of 10 × 2 × 30 mm, with 21 mm of distance between clamps. Storage shear modulus ($G'$) and damping factor (tan $\delta$) were recorded as a function of temperature, from −60°C to 200°C, at a heating rate of 5°C $min^{-1}$. Tensile tests were performed according to the ASTM D1708-02a standard, at room temperature with an Instron 4467 universal testing machine (Buckinghamshire, England) equipped with a 0.5 kN load cell at a crosshead speed of 1 mm $min^{-1}$. Tensile strength was calculated as the average of five replicates.

## RESULTS AND DISCUSSION

*Size Distribution of CNC*

According to DLS results, the size of CNC obtained by acid hydrolysis was in range from 33 to 950 nm [31]. This simple technique consider spherical particles, so that the numbers obtained are comparative, and useful to confirm that the suspension does not have a significant concentration of aggregates, and that the length of the nanocrystals is in the expected order of magnitude.

Size distribution showed that the average size of CNC was 295 nm which coincides with other published results, for example CNC length from 35 to 500 nm and width from 3 to 48 nm have


DOI 10.1002/pen

ID: vedhanarayanan.m Time: 22:12 I Path: //chenas03/Cenpro/ApplicationFiles/Journals/Wiley/PEN#/Vol00000/170022/Comp/APPFile/JW-PEN#170022

COLOR ONLINE AND BW IN PRINT


FIG. 1. Images of composites with different concentrations of CNC, 1 wt% (left) and 2 wt% (right). [Color figure can be viewed at wileyonlinelibrary.com]

been reported in the literature [24, 32, 33]. Additionally, variations between different studies are expected, given the already known dependence of the size of CNC with the source of the cellulosic material and the conditions (temperature, time, stirring methods, etc.) under which the hydrolysis is performed [20].

*Characterization of Nanocomposites*

Before reaction, the liquid mixtures containing different percentages of CNC showed a homogeneous distribution of the nanocrystals in the unreacted liquid mixture. The appearance of the final nanocomposites obtained after compression molding are shown in Fig. 1. The images illustrate that the composites are colored, but transparent even at 2 wt% CNC.

Opacity and colour attributes such as lightness ($L^*$), redness/greenness ($a^*$), and yellowness/blueness ($b^*$) values of PUs with different concentrations of CNC are presented in Table 1. All samples evidenced a tendency to yellowness ($b^*$), as it is observed in the images of Fig. 1, although this value decreased slightly with the incorporation of CNC. Increased lightness ($L^*$) and concomitant decreased opacity values were observed with the incorporation of CNC as compared with PUs matrix. We observed that the $L^*$ and WI values were highest for the 1 wt% CNC composite, suggesting that for this percentage of nanocrystals percolation was reached, as it will be discussed in further sections [29, 34–37].

To evaluate the distribution of nanocrystals in the matrix, the composites were observed in linearly polarized light. Images of the samples are shown in Fig. 2.

The images of Fig. 2 show that the CNCs are uniformly distributed in the PU matrix and that the birefringence of the films increases with the cellulose concentration (0–2 wt%). Figure 3 shows SEM images of the cryo-fracture surfaces of the PU nanocomposites. Comparing the images of the composites to that of the neat PU film, the effect of the CNCs addition can be analyzed. The roughness of the fracture surface increases with the concentration of CNC, which is the result of the crack having to deviate from the original path of fracture when it encounters nanocellulose particles with a higher modulus than the matrix PU. In agreement with the macroscopic observation (Figs. 1 and 2), a homogeneous distribution of CNC in the matrix can be inferred from the fracture surfaces, which implies that there is good compatibility between the cellulose and the PU matrix, and negligible agglomeration. This should be attributed to the polar nature of both, PU and CNCs, and to the interfacial interaction that could include hydrogen-bonds between filler/filler and filler/matrix. Such uniform distribution of the CNC in the matrix is expected to play an important role in improving the mechanical performance of the resulting nanocomposite films, as it will be further discussed [38, 39].

Figure 4 shows the ATR-FTIR spectra of the neat PU, CNC, and PU/CNC 1 wt% nanocomposite. The absence of a peak at 2200 to 2300 $cm^{-1}$ indicates that there is no unreacted isocyanate left in the PU. The peak at 3340 $cm^{-1}$ is assigned to the N-H stretching in hydrogen bonded urethane groups. The IR spectrum of the PU/CNC nanocomposite shows essentially no difference with respect to that of the neat polymer, which is probably due to the low concentration of CNC in the nanocomposites [40]. Regarding the resolution of the FTIR technique to observe CNC in this composition range, other authors have also obtained similar results. The addition of CNC to PU has been detected, according to the literature, by small shifts in the peaks related to H-bonding, which occurs in phase-separated PUs and that is responsible for the particular structure of these polymers. Even in those cases, the shifts were reported at concentrations above 10 wt% of cellulose [39]. In the present case, the results obtained for the crosslinked polyurethane elastomeric

TABLE 1. Optical properties: Colour parameters and opacity of films.

| wt% CNC | $a^*$ | $b^*$ | $L^*$ | Opacity (%) | WI |
|---|---|---|---|---|---|
| 0 | $-2.1 \pm 0.6$ | $51.4 \pm 0.6$ | $71.8 \pm 0.4$ | $11.1 \pm 0.4$ | $41 \pm 3$ |
| 0.5 | $-3.8 \pm 1.7$ | $47.1 \pm 2.4$ | $71.5 \pm 2.9$ | $10.8 \pm 1.5$ | $45 \pm 5$ |
| 1 | $-3.5 \pm 0.8$ | $46.6 \pm 1.1$ | $74.5 \pm 1.0$ | $10.8 \pm 0.6$ | $47 \pm 6$ |
| 2 | $-3.4 \pm 0.8$ | $47.9 \pm 2.4$ | $72.0 \pm 1.0$ | $9.4 \pm 0.3$ | $44 \pm 4$ |



ID: vedhanarayanan.m Time: 22:12 I Path: //chenas03/Cenpro/ApplicationFiles/Journals/Wiley/PEN#/Vol00000/170022/Comp/APPFile/JW-PEN#170022

COLOR ONLINE AND BW IN PRINT

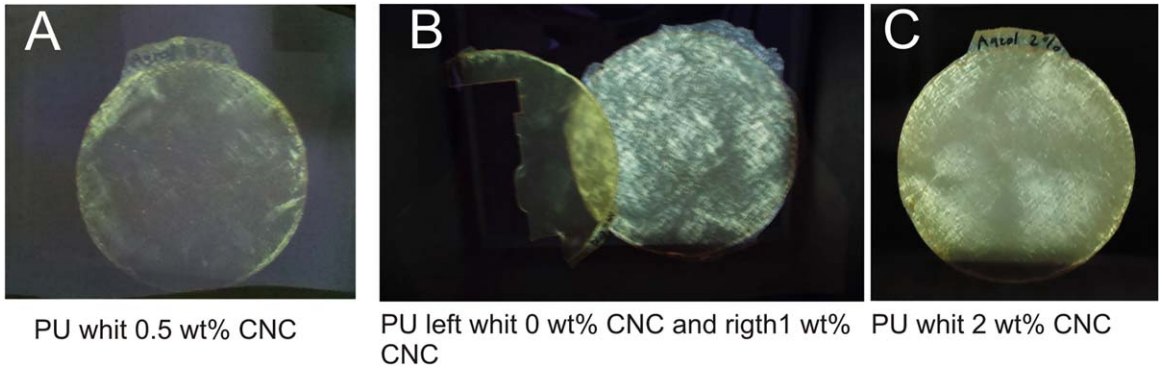


FIG. 2. Images of composite films under cross polarized light. [Color figure can be viewed at wileyonlinelibrary.com]

nanocomposite agree with the observations of Floros et al. [40], who worked with a PU formulation with little H-bonding and that showed no additional FTIR signal after incorporation of nanocellulose, even at the maximum concentration of 2.5 wt% used in their study.

In phase separated PUs, the hydrogen bonds between hard-soft and hard-hard segments promote polymer crystal formation and X-ray diffraction measurements are used to investigate the crystallinity of PU. However, nonsegmented PUs, as the one prepared in this study, do not phase separate and thus, only amorphous X-ray patterns are produced, as depicted in Fig. 5. As it can be observed, all the diffractograms are similar, and show a large broad diffraction peak around $2\theta = 19.58°$ (main diffraction peak), indicating that it is an amorphous PU. This is understandable since it was prepared in one step, without using chain extenders and there is little symmetry in the polymeric isocyanate molecule or in the hydroxylated soybean oil. The similarity of the peaks indicate that the nature of the PU is not affected by the addition of the CNC [41, 42].

The glass transition temperature of the materials ($T_g$) was determined from the DMA results as the temperature value at the maximum in tan $\delta$ and is reported in Table 2. Although other thermal techniques are available to measure $T_g$ (for example DSC), by far the most sensitive technique is DMA [43]. As shown in Table 2, the $T_g$ of the nanocomposites slightly increased with the concentration of CNC, being 31°C for the neat PU and reaching 35°C for the sample containing 2 wt% of CNC. This increase can be related to the increasing restriction

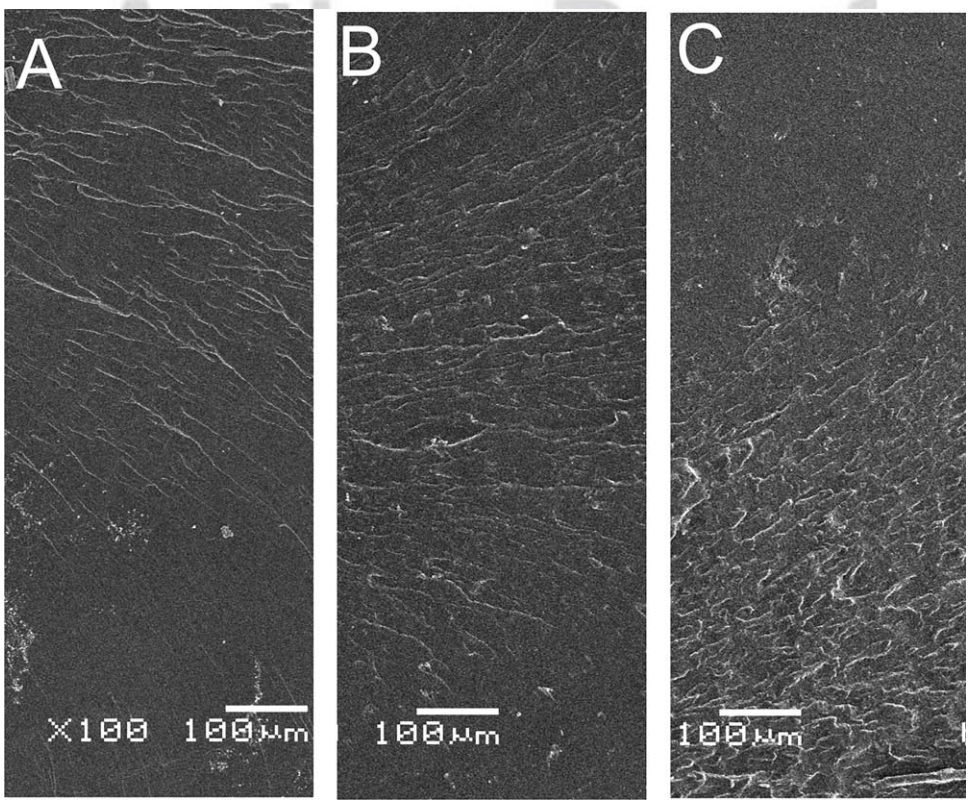


FIG. 3. Images SEM of surface fracture of composite. (A) 0 wt% CNC, (B) 1 wt% CNC, and (C) 2 wt% CNC.



DOI 10.1002/pen

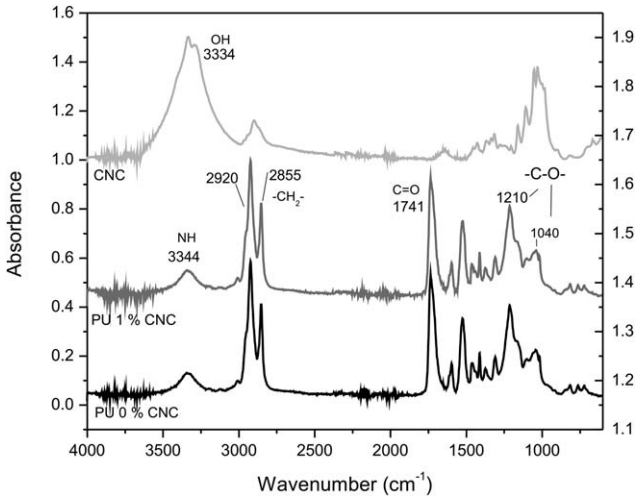


FIG. 4. ATR-FTIR spectra of CNC, neat PU, and PU/CNC nanocomposites with 1% CNC.

of molecular mobility because of the presence of the well dispersed rigid CNC [1].

F6 Figure 6 shows the drop of the storage modulus at the transition region, illustrating also the effect of the CNC addition on the value of the rubbery plateau. For low cellulose contents, the rubbery modulus does not change much, but when a concentration of 2 wt% CNC is reached the rubbery modulus is clearly higher than that of the neat PU.

F7 Figure 7a–d show the TGA and dTG curves for the nanocomposites prepared with different cellulose content under air and nitrogen atmospheres. The curves obtained under air atmosphere revealed that all samples independently of cellulose content presented five main degradation processes. The degradation between 200 and 360°C was assigned to the decomposition of unstable urethane bonds, leading to primary or secondary amines, olefin, and dioxide [44–46]. The weight loss in the temperature range from 360 to 550°C corresponded to chain scission of the hydroxylated soybean oil chain [44, 45]. The thermal degradation of the complex structure of the oil generated two overlapped peaks at 425 and 475°C [44]. In this degradation step, the nanocomposites show a slightly reduced stability (it

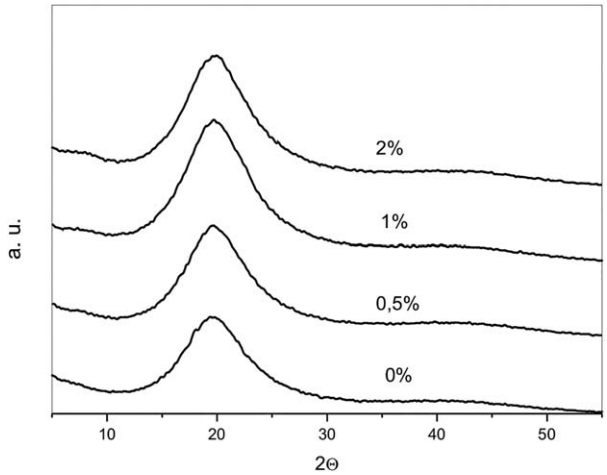


FIG. 5. XRD patterns of PU/CNC composites and PU neat.

TABLE 2. Glass transition temperature and initial decomposition temperature of nanocomposites.

| CNC content (wt%) | $T_g$, °C | $T_{in}$ (°C) $N_2$ | $T_{in}$ (°C) Air |
|---|---|---|---|
| 0 | 31 | 304 | 303 |
| 0.5 | 31 | 310 | 306 |
| 1.0 | 33 | 310 | 307 |
| 2.0 | 35 | 306 | 305 |

starts at ~15°C below the degradation of the neat PU), but there is not much difference between the samples prepared with different CNC concentrations. For temperatures higher than 525°C, combustion processes occurred that involve polymeric fragments and other products generated in the previous degradation steps [44–46]. The small difference observed for the nanocomposites can be linked to the presence of the inorganic sulfate groups on the surface of the CNC.

The thermal degradation curves obtained under nitrogen atmosphere showed even more similar degradation processes, which occurred at higher temperatures than in oxygen atmosphere, as it was expected since the oxidation reactions were restricted. The combustion region at 525 to 700°C did not appear under nitrogen atmosphere.

In both cases, the thermograms of neat PU and nanocomposites were very similar, with a slight improvement at the start of the first degradation step (a shift of 3–5°C towards higher temperature). This means that the crystals were well coated by the polymer and thus, no additional step due or induced by the presence of the CNC was detected by this technique.

### *Tensile Strength and Elastic Modulus*

Klemm et al. [47] found that the optimal enhancement of mechanical properties usually occurs at the point at which just enough reinforcing agent has been added to establish connectivity. For nanocellulose reinforced segmented PU films, Auad et al. obtained approximately 53% increase in tensile modulus

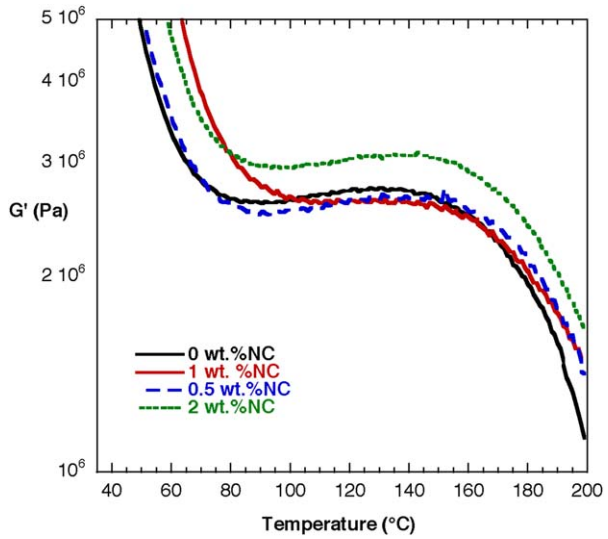


FIG. 6. Storage modulus vs. temperature for the neat PU and cellulose nanocomposites. [Color figure can be viewed at wileyonlinelibrary.com]

COLOR ONLINE AND BW IN PRINT



ID: vedhanarayanan.m Time: 22:12 I Path: //chenas03/Cenpro/ApplicationFiles/Journals/Wiley/PEN#/Vol00000/170022/Comp/APPFile/JW-PEN#170022

COLOR ONLINE AND BW IN PRINT

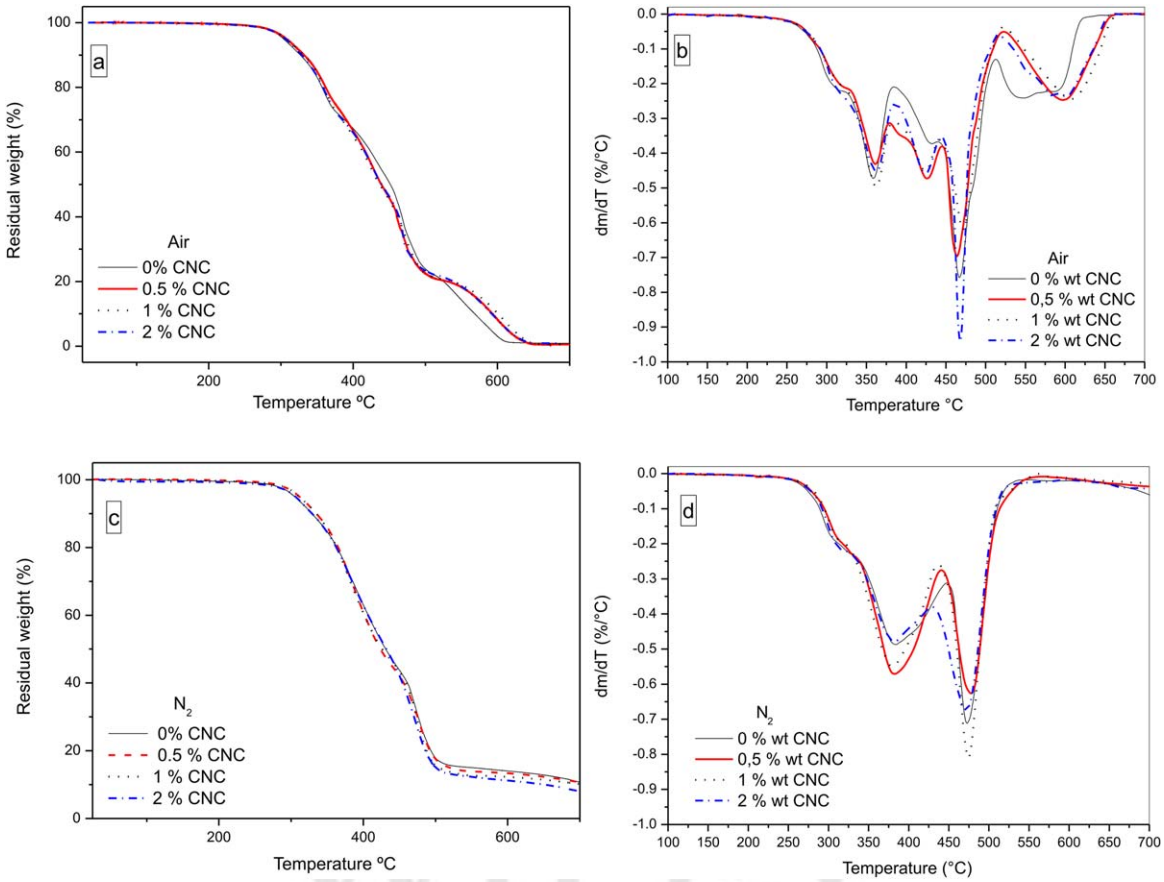


FIG. 7. $T_g$ and dTG curves of PU with different CNC contents (a) and (b) air atmosphere and (c) and (d) nitrogen atmosphere. [Color figure can be viewed at wileyonlinelibrary.com]

Author Proof

by the addition of just 1.0 wt% CNC [48]. Paberza et al. investigated cellulose nanowhiskers as a reinforcing filler in PU foams. Their results showed that tensile modulus decreases by adding 0.5 wt% cellulose nanowhiskers but increases by adding 1 wt% [10]. Also, Cao et al. investigations showed that tensile strength does not increase linearly by adding cellulose-based fibers to PU matrix. The best results were obtained with 0.5 wt% and 1.0 wt% CNC in the PU, but nanocomposite samples with CNC content beyond 1.0 wt% showed a negative effect on mechanical properties [39]. The improved mechanical performance can be related to the compatible nature of the nanocellulose and the PU matrix, that lead to a well-distributed nanofiller, being this a first necessary step to benefit from the use of nanoreinforcements. As it can be inferred from the cited previous publications, when connectivity of the CNC is reached (percolation threshold) a maximum in mechanical properties is achieved because of the contribution of the formed network of rigid CNC. However, when higher concentrations of CNC are used, agglomeration occurs and the reinforcement becomes more similar to that offered by traditional fillers (similarly to what happens with other nanofillers and nanofibers), thus the benefit of the nanosize is lost.

Results of tensile strength and elastic modulus of our investigation are presented in Fig. 8. F8

In the present study, the tensile strength and elastic modulus increased more than two and four times, respectively, by adding 1 wt% CNC to the PU matrix reaching 5.3 MPa of tensile strength and 45 MPa of elastic modulus, values that correspond to a hard elastomeric material [31, 43]. However, samples with 0.5 wt% and 2.0 wt% CNC showed worse performance in mechanical properties than the sample without CNC.

Overall, the change of tensile strength and elastic modulus coincides with other author's results, as described previously. In particular, CNC added in low concentration (0.5 wt%) behave as stress concentrators and point of failure in the composite, they also reacted with the isocyanate but without contributing with cellulose connectivity, since the concentration is below the percolation threshold. At about 1 wt% of CNC the percolation of the system is reached. Although the hydroxyls of the CNC competed with the OH from the polyol in the formation of covalent bonds with the isocyanate, at this concentration level a network of high modulus touching crystals interpenetrates the PU matrix and the mechanical properties are much improved, which is understandable because the sample is at the CNC percolation threshold. Higher concentrations of the crystals result in agglomeration (concentrations above percolation) and thus the properties drop again, since the sample becomes heterogeneous and agglomerates are stress concentrators and points of failure for the material.

These samples show the typical behavior in which the increase in modulus and stress at break is accompanied by the reduction of the elongation at break. However, it should be

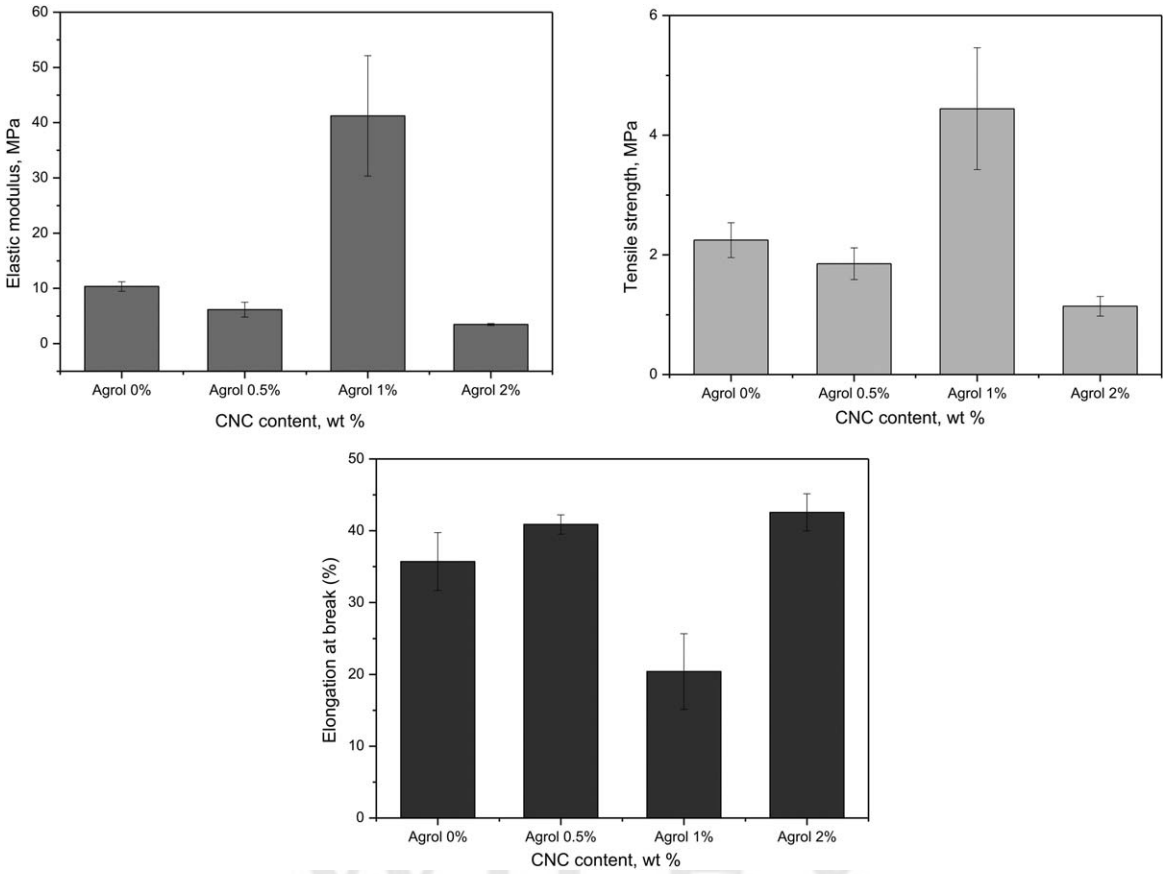


FIG. 8. Elastic modulus, tensile strength and elongation at break of PU composites.

noticed that the behavior of the materials is still elastomeric with the elongation at break of the 1 wt% nanocomposite being 20%.

## CONCLUSIONS

In this work, bio-based PU composites containing CNC were prepared, and the effect of the incorporation of different concentrations of the nanoparticles on the final properties of the PU composites was investigated. At the concentration range of the nanocrystals used (from 0 to 2 wt%) good dispersion of the CNC was achieved, which resulted in transparent films. The use of polarized light proved to be a simple and fast macroscopic tool to determine the adequate distribution of the crystals in the sample.

The $T_g$ of the nanocomposites increased slightly (up to 4°C) with respect to that of the neat PU, reaching 35°C for sample with 2 wt% of CNC. Thermogravimetric analysis showed that the thermal stability of nanocomposites is not changed much by the incorporation of CNC, which also indicates that the crystals are well embedded in the matrix. Results of tensile strength and elastic modulus showed that 1 wt% of CNC is the optimal concentration to improve mechanical properties of PU, with the tensile strength increasing more than two times compared to the result obtained for the neat sample, although the elongation at break was reduced about a 40% with respect to the neat PU. The result is a hard elastomer with a modulus of 43 MPa and elongation at break of 20%. This result was related to this concentration being at about the percolation threshold of the nanocrystals.

Overall, the results indicated that CNC can improve the final properties of PU composites based on hydroxylated soybean oil, if used at the optimum concentration of 1 wt% of cellulose nanocrystals.

## REFERENCES

1. S.H. Park, K.W. Oh, and S.H. Kim, *Compos. Sci. Technol.*, **86**, 82 (2013).
2. M. Ionescu, *Chemistry and Technology of Polyols for Polyurethane*, Smithers Rapra Press, Shawbury, Shrewsbury, Shropshire, UK (2008).
3. Y. Chen, C. Liu, P.R. Chang, D.P. Anderson, and M.A. Huneault, *Polym. Eng. Sci.*, **49**, 369 (2009).
4. A. Noreen, K.M. Zia, M. Zuber, S. Tabasum, and A.M. Zahoor, *Prog. Org. Coat.*, **91**, 25 (2016).
5. R. Tanaka, S. Hirose, and H. Hatakeyama, *Bioresour. Technol.*, **99**, 3810 (2008).
6. N.P.N. Pauzi, R.A. Majid, M.H. Dzulkifli, and M.Y. Yahya, *Compos. B*, **67**, 521 (2014).
7. V.M. Wik, M.I. Aranguren, and M.A. Mosiewicki, *Polym. Eng. Sci.*, **51**, 1389 (2011).
8. U. Stirna, A. Fridrihsone, B. Lazdiņa, M. Misāne, and D.J. Vilsone, *Polym. Environ.*, **21**, 952 (2013).
9. M. Kurańska, M. Prociak, M. Kirpluks, and U. Cabulis, *Ind. Crops. Prod.*, **74**, 849 (2015).



ID: vedhanarayanan.m Time: 22:13 I Path: //chenas03/Cenpro/ApplicationFiles/Journals/Wiley/PEN#/Vol00000/170022/Comp/APPFile/JW-PEN#170022

10. A. Paberza, A. Fridrihsone-Girone, A. Abolins, and U. Cabulis, *Polimery*, **60**, 572 (2015).
11. U. Stirna, U. Cabulis, and I. Beverte, *J. Cell. Plast.*, **44**, 139 (2008).
12. D. Ji, Z. Fang, W. He, Z. Luo, X. Jiang, T. Wang, and K. Guo, *Ind. Crops. Prod.*, **74**, 76 (2015).
13. A. Lee, and Y. Deng, *Eur. Polym. J.*, **63**, 67 (2015).
14. L. Zhang, M. Zhang, L. Hu, and Y. Zhou, *Ind. Crops. Prod.*, **52**, 380 (2014).
15. C. Fu, Z. Yang, Z. Zheng, and L. Shen, *Prog. Org. Coat.*, **77**, 124 (2014).
16. B. Das, U. Konwar, M. Mandal, and N. Karak, *Ind. Crops. Prod.*, **44**, 396 (2013).
17. S.A. Seyedmehdi, H. Zhang, and J. Zhu, *Polym. Eng. Sci.*, **54**, 1120 (2014).
18. Y. Li and A. Ragauskas, "Cap.2: Cellulose Nano Whiskers as a Reinforcing Filler in Polyurethanes," in *Advances in Diverse Industrial Applications of Nanocomposites*, R. Boreddy, Ed. (2011). AQ2
19. M.L. Auad, M.A. Mosiewicki, T. Richardson, M.I. Aranguren, and N.E. Marcovich, *J. Appl. Polym. Sci.*, **115**, 1215 (2010).
20. M.A. Mosiewicki, P. Rojek, S. Michałowski, M.I. Aranguren, and A. Prociak, *J. Appl. Polym. Sci.*, **132**, 41602 (2015).
21. R.J. Moon, A. Martini, J. Nairn, J. Simonsen, and J. Youngblood, *Chem. Soc. Rev.*, **7**, 3941 (2011).
22. J. Bras, M.L. Hassan, C. Buzesse, E. Hassan, N. El-Wakil, and A. Dufresne, *Ind. Crops Prod.*, **32**, 627 (2010).
23. Y. Habibi, L.A. Lucia, and O.J. Rojas, *Chem. Rev.*, **110**, 3479 (2010).
24. S. Elazzouzi-Hafraoui, Y. Nishiyama, J.L. Putaux, L. Heux, F. Dubreuil, and C. Rochas, *Biomacromolecules*, **9**, 57 (2008).
25. J.K. Pandey, A.N. Nakagaito, and H. Takagi, *Polym. Eng. Sci.*, **53**, 1 (2013).
26. K. Lee, Y. Aitomäki, L.A. Berglund, K. Oksman, and A. Bismarck, *Compos. Sci. Technol.*, **105**, 15 (2014).
27. A. Vatansever, H. Dogan, T. Inan, S. Sezer, and A. Sirkecioglu, *Polym. Eng. Sci.*, **55**, 2922 (2015).
28. A. Casariego, B.W.S. Souza, M.A. Cerqueira, J.A. Teixeira, L. Cruz, R. Díaz, and A.A. Vicente, *Food Hydrocolloids*, **23**, 1895 (2009).
29. M. Pereda, M.I. Aranguren, and N.E. Marcovich, *J. Appl. Polym. Sci.*, **107**, 1080 (2008).
30. P.M. Stefani, V. Cyras, A. Tejeira Barchi, and A. Vazquez, *J. Appl. Polym. Sci.*, **99**, 2857 (2006).
31. A Ivdre, V Mucci, P M Stefani, M I Aranguren and U Cabulis, "Nanocellulose reinforced polyurethane obtained from hydroxylated soybean oil," in *Baltic Polymer Symposium* 2015, *IOP Conference Series: Materials Science and Engineering* (2015) 111 012011 doi:10.1088/1757-899X/111/1/012011.
32. L. Pranger, and R. Tannenbaum, *Macromolecules*, **41**, 8682 (2008).
33. J.R. Capadona, K. Shanmuganathan, S. Trittschuh, S. Seidel, S.J. Rowan, and C. Weder, *Biomacromolecules*, **10**, 712 (2009).
34. M. Pereda, A.G. Ponce, N.E. Marcovich, R.A. Ruseckaite, and J.F. Martucci, *Food Hydrocolloids*, **25**, 1372 (2011).
35. C. Peña-Rodriguez, J.F. Martucci, L.M. Neira, A. Arbelaiz, A. Eceiza, and R.A. Ruseckaite, *Food Sci. Technol. Int.*, **21**, 221 (2015).
36. N. Auclair, A. Kaboorani, B. Riedl, and V. Landry, *Ind. Crops Prod.*, **82**, 118 (2016).
37. X. Li, C. Qiu, N. Ji, C. Sun, L. Xiong, and Q. Sun, *Carbohydr. Polym.*, **121**, 155 (2015).
38. H. Liu, S. Cui, S. Shang, D. Wang, and J. Song, *Carbohydr. Polym.*, **96**, 510 (2013).
39. X. Cao, H. Dong, and C.M. Li, *Biomacromolecules*, **8**, 899 (2007).
40. M. Floros, L. Hojabri, E. Abrahama, J. Jose, S. Thomas, L. Pothan, A. Lopes Leao, and S. Narine, *Polym. Degrad. Stab.*, **97**, 1970 (2012).
41. L. Lei, Y. Zhang, C. Ou, Z. Xia, and L. Zhong, *Prog. Org. Coat.*, **92**, 85 (2016).
42. J. Huang, J.W. Zou, P.R. Chang, J.H. Yu, and A. Dufresne, *Express Polym. Lett.*, **5**, 362 (2011).
43. *Thermal Analysis and Reology*, http://www.tainstruments.com/pdf/literature/TS64.pdf (accessed date September 14, 2015).
44. Y. Lu, and R.C. Larock, *Prog. Org. Coat.*, **69**, 31 (2010).
45. C. Zhang, S.A. Madbouly, and M.E. Kessler, *ACS Appl. Mater. Interfaces*, **7**, 1226 (2015).
46. Z.S. Petrovic, L. Yang, A. Zlatanic, W. Zhang, and I. Javni, *J. Appl. Polym. Sci.*, **105**, 2717 (2007).
47. D. Klemm, F. Kramer, S. Moritz, T. Lindstrom, M. Ankerfors, D. Gray, and A. Dorris, *Angew. Chem. Int.*, **50**, 5438 (2011).
48. M.L. Auad, V.S. Contos, S. Nutt, M.I. Aranguren, and N.E. Marcovich, *Polym. Int.*, **57**, 651 (2008).
49. M. I. Aranguren, N. E. Marcovich, M. A. Mosiewicki. "Mechanical Performance of PU based bio-composites," in *Bio-composites: Design and Mechanical Performance*, M. Misra, J. K. Pandey, and A. K. Mohanty, Eds., Woodhead Publishing Ltd., Chapter , 465 (2015). ISBN 978-178242394-2; 978-178242373-7 AQ3 AQ4


WILEY Author Proof

[AQ1] Kindly provide the department/division name for the first and second affiliations.

[AQ2] Kindly provide the publisher name and location details for the Refs. 18 and 31.

[AQ3] Kindly provide the publisher location details for the Ref. 49.

[AQ4] Please note that Ref. 49 has not been cited anywhere in the text. Kindly cite it or delete the same from the list.

[AQ5] Please confirm whether the color figures should be reproduced in color or black and white in the print version. If the color figures must be reproduced in color in the print version, please fill the color charge form immediately and return to Production Editor. Or else, the color figures for your article will appear in color in the online version only.

AQ6: Please confirm that given names (red) and surnames/family names (green) have been identified correctly.

Please confirm that the funding sponsor list below was correctly extracted from your article: that it includes all funders and that the text has been matched to the correct FundRef Registry organization names. If a name was not found in the FundRef registry, it may be not the canonical name form or it may be a program name rather than an organization name or it may be an organization not yet included in FundRef Registry. If you know of another name form or a parent organization name for a not found item on this list below, please share that information.

| FundRef name | FundRef Organization Name (Country) | FundRef DOI | Grant IDs |
|---|---|---|---|
| BIOPURFIL Project | [NOT FOUND IN FUNDREF REGISTRY] | | PIRSES-GA-2012-318996 by the EC through the FP7 |
| National Research Council of Republic Argentina (CONICET) | Consejo Nacional de Investigaciones Científicas y Técnicas | 10.13039/501100002923 | PIP 0866 |
| Science and Technology National Promotion Agency (ANPCyT) | [NOT FOUND IN FUNDREF REGISTRY] | | PICT140732 |
| National University of Mar del Plata (UNMdP) | Jesus University<br>Maryland Sea Grant, University of Maryland<br>Syddansk Universitet<br>Universiti Teknologi MARA<br>University of Maryland<br>[NOT FOUND IN FUNDREF REGISTRY] | | 15/G430-ING436/15 |

WILEY Author Proof